

11<sup>th</sup> U. S. National Combustion Meeting  
Organized by the Western States Section of the Combustion Institute  
March 24–27, 2019  
Pasadena, California

## R-152a/air and R-134a/oxygen constant volume spherical flame burning velocity measurements

*Robert R. Burrell\*, Michael J. Hegetschweiler, Donald R. Burgess Jr.,  
Jeffrey A. Manion, Valeri I. Babushok, Gregory T. Linteris*

*Energy and Environment Division, National Institute of Standards and Technology,  
Gaithersburg, Maryland, 20899, USA*

*\*Corresponding Author Email: Linteris@nist.gov*

**Abstract:** Many presently used refrigerants are non-flammable but are being phased out due to concerns about their high global warming potential (GWP). Replacements with low GWP exist but tend to be flammable with a maximum burning velocity in air between 1 cm/s and 40 cm/s, depending on molecular structure. Flammable refrigerants are a rising challenge for industry, which can benefit from predictive tools for ranking refrigerant flammability based on fundamentals. This work reports experimental burning velocities via pressure rise measurements in a constant volume spherical chamber interpreted with the aid of a thermodynamic spherical flame model. Flames of R-152a/air and R-134a/oxygen mixtures over a range of equivalence ratios provide experimental burning velocities for unburned gas conditions at 298 K and 0.101 MPa, and at 375 K and 0.253 MPa. This work supports the development of validated and optimized kinetic models for the combustion of refrigerants at conditions relevant to fire safety.

**Keywords:** *Refrigerant Flammability; Spherical Flame; 1,1 Difluoroethane; 1,1,1,2-Tetrafluoroethane*

### 1. Introduction

The world is phasing down use of refrigerants with high global warming potential (GWP). One way to limit GWP is to use refrigerants with higher reactivity and shorter atmospheric half-life. Higher reactivity also often implies greater flammability in air. Flammable refrigerants are a rising challenge for the heating, ventilation, air-conditioning, and refrigeration industry, which can benefit from tools for predicting flammability characteristic based on fundamentals. Efforts are underway at the National Institute of Standards and Technology (NIST) to develop a comprehensive chemical kinetic model for refrigerant combustion validated against fundamental burning velocity ( $S_u^0$ ) data. The definition for  $S_u^0$  applies to flames that are freely propagating, laminar, one-dimensional, planar, adiabatic, and stretch free. In laboratory flames subject to flame stretch and/or heat loss, the burning velocity ( $S_u$ ) can deviate from the ideal  $S_u^0$ .

Combustion kinetic models are hierarchical in nature; reactions for small chemical species form a subset of those for larger species. For example, methane combustion reactions are a subset of

those for ethane and higher alkanes. The authors previously developed a kinetic model for R-32 (difluoromethane) combustion from a critical evaluation of reaction rates and validated it against  $S_u^0$  measurements [1-3]. The authors now turn attention to the two-carbon refrigerants R-134a (1,1,1,2-tetrafluoroethane) and R-152a (1,1-difluoroethane). R-134a is a widely used working fluid for stationary refrigeration and automobile air-conditioning systems. It has a low H/F atom ratio of  $\frac{1}{2}$ , resulting in low overall reactivity and non-flammability at typical atmospheric conditions. There are no known  $S_u^0$  measurements for flames of a single-component R-134a fuel. It has a high GWP (1300 times that of  $\text{CO}_2$ ) and its use is being phased down. R-152a is not widely used as a refrigerant, but it offers similar thermodynamic cycle performance as R-134a. It has an H/F ratio of 2 which results in moderate flame reactivity and a much lower GWP (140 times that of  $\text{CO}_2$ ). Measurements by Takizawa et al. [4] and Moghaddas et al. [5] using constant volume method spherical flames indicate a maximum R-152a/air  $S_u^0$  at standard conditions near 23 cm/s.

The goal of this work is to further support development and validation of the NIST refrigerant combustion kinetic model with  $S_u^0$  data for R-134a/ $\text{O}_2$  and R-152a/air mixtures. This is achieved by taking pressure rise measurements of outwardly propagating spherical flames in a constant volume spherical chamber.  $S_u$  is inferred from the measured pressure history using a thermodynamic model to determine the relationship between chamber pressure and flame radius. The influence of initial transients, flame instabilities, and flame-wall interactions on data reduction are investigated. Data not affected by these influences are used to produce experimental  $S_u^0$  values for R-134a/ $\text{O}_2$  mixtures over a range of fuel-oxidizer equivalence ratios ( $\phi$ ) from  $0.6 \leq \phi \leq 1.2$  at (298 K, 0.101 MPa) and for R-152a/air mixtures over  $0.8 \leq \phi \leq 1.3$  at (298 K, 0.101 MPa) and (375 K, 0.253 MPa).

## 2. Experimental Methods

Measurements were performed using the 15.24 cm inner diameter spherical chamber described previously [3, 6, 7]. Reactants were R-134a, R-152a (99.5 %),  $\text{O}_2$  (99.5 %), and house filtered/dried air. The chamber was evacuated to below 67 Pa for 5 minutes, then reactants were added by partial pressure as measured with an absolute pressure transducer (Omega PX811) calibrated to an in-house reference (Baratron 627D) until the desired  $\phi$  was achieved. R-134a/ $\text{O}_2$  mixtures were prepared at an initial state  $T_i = 298$  K and  $P_i = 0.1013$  MPa for  $0.6 \leq \phi \leq 1.2$ . R-152a/air mixtures were prepared for multiple initial states with  $T_i = 298$  K and  $P_i = 0.0880$  MPa, 0.1013 MPa, and 0.1147 MPa. Variability in  $T_i$  was  $\pm 2$  K and in  $P_i$  was  $\pm 0.0001$  MPa. Mixtures were given 5 minutes to settle then centrally ignited by a spark powered by either a 5 nF or 10 nF capacitor bank charged to between 6 kV to 14 kV. Estimated ignition energies range between 0.31 mJ to 5.6 mJ [8]. Pressure rise in the chamber caused by the outward expansion of a spherical flame was recorded using a piezoelectric sensor at 10 kHz in R-134a/ $\text{O}_2$  mixtures and 5 kHz in R-152a/air mixtures. During post-processing, the effective data rate was set to 1.667 kHz to reduce the relative effect of measurement noise. A previous uncertainty analysis of the present system [7] indicates the maximum  $S_u$  uncertainty for a single point measurement is  $\pm 12$  % ( $2\sigma$ ) and occurs in off-stoichiometric mixtures, which is about  $\pm 1$  cm/s in R-134a/ $\text{O}_2$  flames and  $\pm 2$  cm/s in R-152a/air flames.

### 3. Data Reduction

Given that only the pressure ( $P$ ) vs. time ( $t$ ) history is measured, determining the corresponding  $S_u$  requires modeling to relate the flame radius ( $R_f$ ) to  $P$ . This was achieved using a two-zone, thermodynamic, spherical flame model [6, 9, 10], with thermodynamic data for 13 species ( $O_2$ ,  $N_2$ ,  $CO_2$ ,  $HF$ ,  $CO$ ,  $H_2O$ ,  $H_2$ ,  $CF_4$ ,  $CF_2O$ ,  $OH$ ,  $O$ ,  $F$ , and  $H$ ) taken from the NASA CEA2 database [11, 12], and heats of formation for R-134a and R-152a of -910 kJ/mol and -512 kJ/mol, respectively, taken from the NIST refrigerant combustion kinetic model. The two-zone model divides the chamber into adiabatic burned and unburned zones, each with uniform temperature and composition separated by a smooth, spherical, and infinitesimally thin flame front. No reactions occur in the unburned gas and the burned gas is at chemical equilibrium. The pressure is spatially uniform but rises in time due to isentropic compression from the expanding flame.

The model divides the spherical volume of reactants at initial state ( $T_i$ ,  $P_i$ ) into a series of shells spaced to correspond with the distance the flame propagates over a segment of the measured pressure. A shell is burned by computing the equilibrium state of the unburned reactants for constant  $P$  and enthalpy. This increases the burned shell volume and temperature ( $T_b$ ), but the unburned shell volume and temperature ( $T_u$ ) are unchanged. Both volumes are simultaneously isentropically compressed to match the chamber volume, which increases  $T_u$  and  $P$ . In practice, this is achieved by fixing  $P$  to the measured values and iteratively solving for  $T_b$  and the burned gas mass fraction ( $\chi_b$ ). The flame radius ( $R_f$ ) is calculated as  $R_f = R_w[1 - (1 - \chi_b)(P_i/P)^{\frac{1}{\gamma_u}}]^{\frac{1}{3}}$ , where  $R_w$  is the chamber wall radius and  $\gamma_u$  is the unburned gas specific heat ratio. Finally, the experimental  $S_u$  values were calculated:

$$S_u = \frac{R_w}{3} \left( \frac{R_w}{R_f} \right)^2 \left( \frac{P_i}{P} \right)^{\frac{1}{\gamma_u}} \left( \frac{d\chi_b}{dt} \right) \quad \text{Eqn. 1}$$

which depends on measured  $P(t)$  and modeled components  $\gamma_u(P)$  and  $\chi_b(P)$ . The resulting  $S_u$  evolves in time along an isentrope in  $(T_u, P)$  space unique to the initial state of the reactants.

The data for a given  $\phi$  were fit to a power law surface,  $\widehat{S}_u = S_{u,ref}(T_u/T_{u,ref})^a(P/P_{ref})^b$ , where  $S_{u,ref}$  is the  $S_u$  value of the fit surface at reference unburned gas conditions ( $T_{u,ref}$ ,  $P_{ref}$ ) and the exponents  $a$  and  $b$  are the temperature and pressure dependence of  $S_u$  as determined by the fitting process. An example  $\widehat{S}_u$  surface is shown for R-152a/air at  $\phi = 1.1$  in Fig. 1 with the corresponding  $S_u$  data (orange circles) also shown projected onto each coordinate plane (black dots). Two  $(T_u, P)$  states are marked (blue squares) in Fig. 1 at which experimental  $S_u^0$  values are provided for R-152a/air mixtures, (298 K, 0.101 MPa), which results from extrapolation, and (375 K, 0.253 MPa) obtained through interpolation.

Choosing appropriate  $(T_u, P)$  conditions for interpolation or extrapolation is dictated by the experimental range. Consider the  $(T_u, P)$  plane in Fig. 1 which shows the unburned gas histories

of R-152a/air flames at three initial pressures. A wide range of conditions can be selected that are bounded by the experimental isentropes, e.g., via interpolation to (375 K, 0.253 MPa). On the other hand, R-134a/air  $S_u$  curves (not shown) were prepared at only one initial pressure. This situation is analogous to only using one of the three R-152a/air ( $T_u, P$ ) histories to fit  $\widehat{S}_u$ . A single  $S_u$  curve is two-dimensional and does not constrain the surface fit in the direction orthogonal to the curve. However, the fit remains well-constrained in the direction tangential to the  $S_u$  curve, thus interpolation or extrapolation can still be performed along the isentropes, e.g., via extrapolation to the initial condition (298 K, 0.101 MPa).

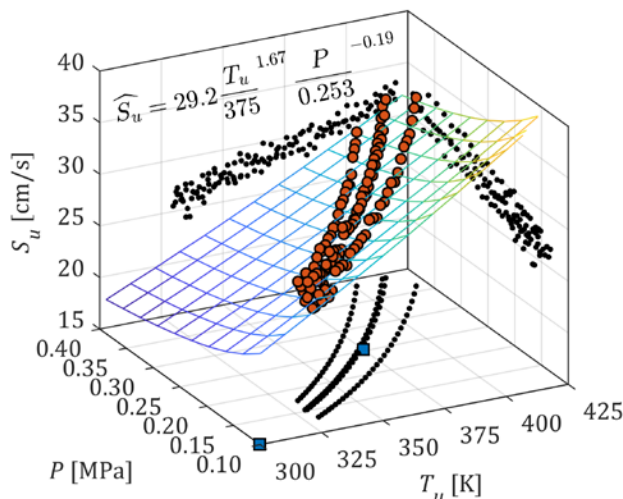


Fig. 1: Comparison of fitted  $\widehat{S}_u$  surface (mesh) and experimental  $S_u$  values (orange circles) for R-152a/air at  $\phi = 1.1$  with the locations of conditions used to report  $S_u^0$  (blue squares) and projections of  $S_u$  data onto coordinate planes (black dots).

#### 4. Results and Discussion

Determining the proper range of flame data for fitting surfaces is a matter of interpretation. Fig. 2 shows examples of experimental  $S_u$  data for R-134a/O<sub>2</sub> mixtures projected onto the ( $T_u, S_u$ ) plane for clarity. Starting near the initial condition of  $T_u = T_i = 298$  K, the flame radius is small and the  $S_u$  noise is initially large and then decays. As the flame sphere grows,  $T_u$  increases, noise reduces, and an increasing  $S_u$  trend forms for  $T_u > 310$  K, which become quasi-linear for  $T_u > 320$  K. For  $T_u > 375$  K, there is apparent flame acceleration initiating at lower  $T_u$  for richer mixtures. The reason for this is believed to be the diffusive-thermal instability [13] known (in rich hydrocarbon/air flames) to cause a non-smooth, cellular flame that leads to enhanced overall mass burning rates. In all cases,  $S_u$  decreases as the flame becomes large enough to quench near the chamber walls.

The characteristics of experimental  $S_u$  values in R-152a/air flames, shown in Fig. 3, are broadly similar to those identified for R-134a/O<sub>2</sub> flames. There is an initial period of high measurement

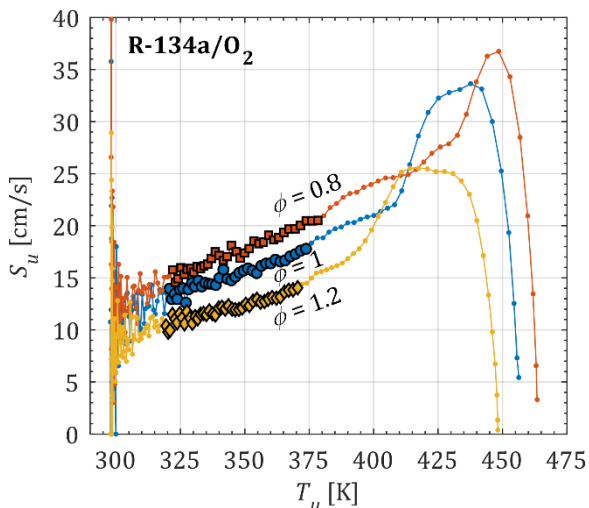


Fig. 2: Experimental  $S_u$  values for initial conditions (298 K, 0.101 MPa).

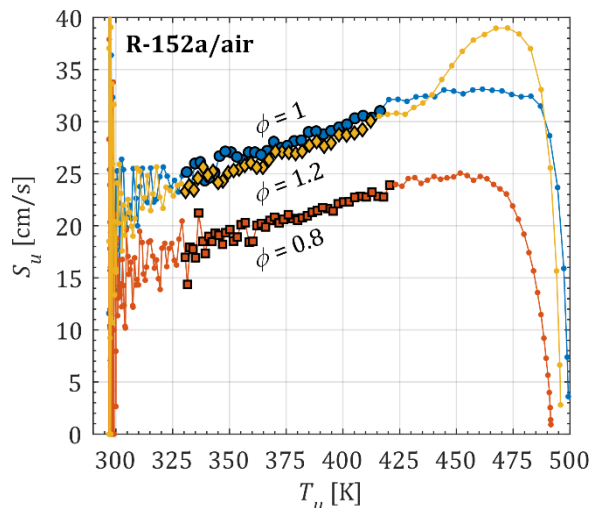


Fig. 3: Experimental  $S_u$  values for initial conditions (298 K, 0.101 MPa).

noise followed by quasi-linear  $S_u(T_u)$  response culminating with  $S_u$  going to zero. Evidence for cellular instability was observed at  $\phi = 1.2$  but not in leaner mixtures. The reasons for the reduced occurrence of instabilities in R-152a/air mixtures are not presently clear. One possibility is lower flame temperatures for R-152a/air mixtures than R-134a/O<sub>2</sub>. For example, at  $P = 4P_i$  for the  $\phi = 1$  curves shown in Figs. 2 and 3, the R-152a/air unburned mixture is near 420 K with a calculated adiabatic flame temperature of 2310 K while the R-134a/O<sub>2</sub> reactants are only near 370 K with a higher adiabatic flame temperature above 2400 K. Higher flame temperatures drive greater unburned-to-burned mass density ratios across the flame front, promoting cell formation via hydrodynamic instability [13].

Taking the raw  $S_u$  data characteristics into consideration, some guidelines can be established for acceptable  $S_u$  data. Initial transients, cellular instabilities, and flame-wall interactions should be avoided by looking for a quasi-linearly increasing  $S_u(T_u)$  trend at intermediate  $T_u$ . It is convenient to formalize the conditions in terms of  $P$ , which is the only measured variable. The initial transients were avoided by eliminating data with  $P < 1.5P_i$ . Cellular instabilities and flame-wall interactions were avoided by eliminating data with  $P > 4P_i$ . Data conforming to these pressure conditions are denoted by symbols with black borders in Fig. 2 and Fig. 3.

Experimental  $S_u^0$  values derived from  $\widehat{S}_u$  fits are shown in Fig. 4 for R-134a/O<sub>2</sub> flames at (298 K, 0.101 MPa). A maximum  $S_u^0$  of 10.8 cm/s was observed near  $\phi = 0.7$  (uncertainties,  $1\sigma$ , are due to the surface fit and extrapolation). To the authors' knowledge, these are the first  $S_u^0$  measurements reported in flames using a single-component R-134a fuel. Due to the relatively low burning velocities, the present  $S_u^0$  values are likely to be influenced by burned gas thermal radiation, which has not presently been addressed. The absence of N<sub>2</sub> in the oxidizer increases the concentration of the emitting/absorbing species. Radiation corrections in R-32/air flames [3]

increased  $S_u^0$  by about 15 %. Future work will quantify the impact of thermal radiation in these flames.

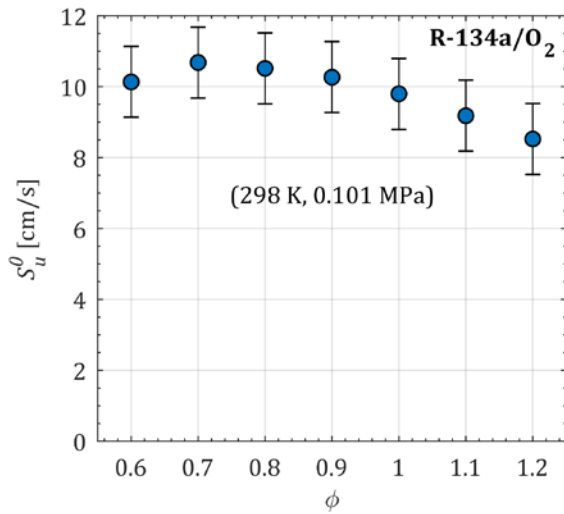


Fig. 4: Experimental  $S_u^0$  values for R-134a/O<sub>2</sub> mixtures.

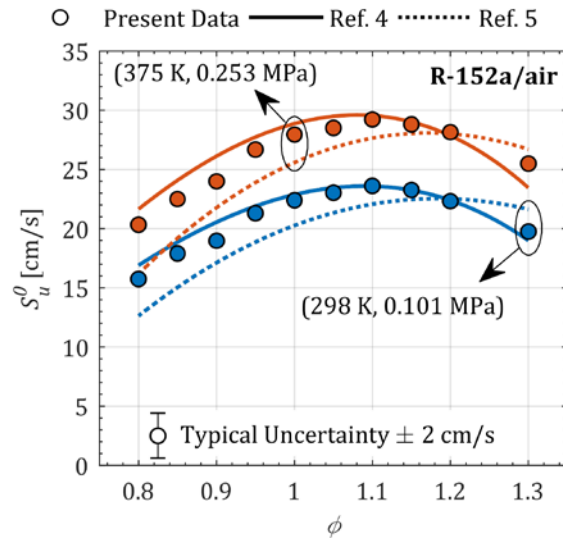


Fig. 5: Experimental  $S_u^0$  values for R-152a/air mixtures with literature values.

Experimental  $S_u^0$  values derived from  $\widehat{S}_u$  fits are shown in Fig. 5 for R-152a/air flames at and (375 K, 0.253 MPa) along with correlations from measurements by Takizawa et al. [4] and Moghaddas et al. [5]. A maximum experimental  $S_u^0$  of 24 cm/s was observed near  $\phi = 1.1$  at (298 K, 0.101 MPa), increasing to 29 cm/s at (375 K, 0.253 MPa). The magnitude of  $S_u^0$  is less than seen in hydrocarbon/air flames and there is less variation of  $S_u^0$  with  $\phi$ , although the shape is similar. The similarities to hydrocarbon/air flames may be attributed to the refrigerant H/F ratio significantly above unity. Although burned gas thermal radiation corrections have not been made, the relatively high  $S_u^0$  values for R-152a/air mixtures suggest that the correction will be small. Neither Refs. 4 nor 5 applied radiation corrections, so a straightforward comparison to the present data is possible. Generally, the present burning velocities compare well with the experimental correlations from Ref. 4, but are slightly slower on the lean side and faster on the rich side. The experimental correlation values from Ref. 5 are lower in maximum value, and the  $S_u^0$  vs  $\phi$  shape is shifted toward richer mixtures compared to both Ref. 4 and the present  $S_u^0$  values.

## 5. Conclusions

Experimental burning velocities of R-152/air and R-134a/O<sub>2</sub> mixtures were obtained by measuring the pressure rise caused by a spherically expanding flame in a constant volume spherical chamber. Burning velocities were extracted from the measured pressure traces using a two-zone thermodynamic model to obtain the relationship between the chamber pressure and the flame radius. Data taken at early times were deemed unreliable due to high measurement noise and data at late times were affected by flame-wall interactions. For richer flames, a rapid burning velocity increase at higher temperatures was believed to be due to the onset of flame instabilities. These data were eliminated when deriving experimental burning velocities. Stretch-free fundamental

burning velocities of R-134a/O<sub>2</sub> flames were reported for equivalence ratios from 0.6 to 1.2 at 298 K and 0.101 MPa. The data indicate a peak fundamental burning velocity of about 10 cm/s for lean equivalence ratios near 0.7. Burning velocities of R-152a/air flames were reported for equivalence ratios of 0.8 to 1.3 at 298 K and 0.101 MPa and 375 K and 0.253 MPa. The data indicate a peak fundamental burning velocity at 298 K and 0.101 MPa of about 24 cm/s near an equivalence ratio of 1.1. Future work will quantify the influence of flame stretch and burned gas thermal radiation on measurements.

## 6. Acknowledgements

This work was supported by the Buildings Technologies Office of the U.S. Department of Energy, Office of Energy Efficiency and Renewable Energy under contract no. DO-EE0007615 with Antonio Bouza serving as Project Manager. Dr. Burrell was supported by a NIST National Research Council postdoctoral research associateship.

## 7. References

- [1] D. R. Burgess Jr, J. A. Manion, R. R. Burrell, V. I. Babushok, M. J. Hegetschweiler and G. T. Linteris, Development and Validation of a Mechanism for Flame Propagation in R-32/Air Mixtures, Spring Meetings of the Eastern States Section of the Combustion Institute (2018).
- [2] D. R. Burgess Jr, J. A. Manion, R. R. Burrell, V. I. Babushok, M. J. Hegetschweiler and G. T. Linteris, Validated model for burning velocities of R-32/O<sub>2</sub>/N<sub>2</sub> Mixtures over a wide range of conditions, 11th US National Combustion Meeting (2019).
- [3] R. R. Burrell, J. L. Pagliaro and G. T. Linteris, Effects of stretch and thermal radiation on difluoromethane/air burning velocity measurements in constant volume spherically expanding flames, *Proceed. Combust. Inst.* (2019) 4231-4238.
- [4] K. Takizawa, A. Takahashi, K. Tokuhashi, S. Kondo and A. Sekiya, Burning velocity measurement of fluorinated compounds by the spherical-vessel method, *Combust. Flame* (2005) 298-307.
- [5] A. Moghaddas, C. Bennett, E. Rokni and H. Metghalchi, Laminar burning speeds and flame structures of mixtures of difluoromethane (HFC-32) and 1,1-difluoroethane (HFC-152a) with air at elevated temperatures and pressures, *HVAC&R Res.* (2014) 42-50.
- [6] J. L. Pagliaro, G. T. Linteris, P. B. Sunderland and P. T. Baker, Combustion inhibition and enhancement of premixed methane-air flames by halon replacements, *Combust. Flame* (2015) 41-49.
- [7] J. L. Pagliaro, G. T. Linteris and V. I. Babushok, Premixed flame inhibition by C<sub>2</sub>HF<sub>3</sub>Cl<sub>2</sub> and C<sub>2</sub>HF<sub>5</sub>, *Combust. Flame* (2016) 54-65.

Sub Topic: Laminar Flames

[8] J. L. Pagliaro, Inhibition of laminar premixed flames by Halon 1301 Alternatives, Thesis, Department of Fire Protection Engineering, University of Maryland, College Park, 2015.

[9] M. Metghalchi and J. C. Keck, Laminar burning velocity of propane-air mixtures at high temperature and pressure, *Combust. Flame* (1980) 143-154.

[10] P. G. Hill and J. Hung, Laminar Burning Velocities of Stoichiometric Mixtures of Methane with Propane and Ethane Additives, *Combust. Sci. Technol.* (1988) 7-30.

[11] S. Gordon and B. J. McBride, Computer program for calculation of complex chemical equilibrium compositions and applications, Report No. NASA Reference Publication 1311, NASA Glenn Research Center, Cleveland, OH, USA, 1996.

[12] NASA Chemical Equilibrium Solver with Applications (CEA), NASA Glenn Research Center, Cleveland, OH, USA, <https://www.grc.nasa.gov/www/CEAWeb/>, updated: Feb. 4, 2016.

[13] M. Matalon, Flame dynamics, *Proceed. Combust. Inst.* (2009) 57-82.